ORIGINAL RESEARCH ARTICLE

Study on Selective Leaching of Copper and Simultaneous Precipitation of Iron in Polymetallic Complex Chalcopyrite by Hydrothermal Leaching Under Oxygen Pressure

JIAJUN XI, GUANGXIONG JI, YALONG LIAO, QINGFENG LIU, and YUE WU

Due to the increasing complexity and dilution of copper resources, a large number of refractory polymetallic complex chalcopyrite are produced. In this study for resolving puzzle in oxygen pressure acid leaching of polymetallic complex chalcopyrite, such as prone to produce dangerous solid wastes like lead jarosite and high iron content in leaching solution, the technology of hydrothermal leaching under oxygen pressure without acid is proposed to extract copper efficiently and selectively and to precipitate iron by hematite process simultaneously. The results show that under the experimental conditions of initial sulfuric acid concentration of 0 g/L, reaction temperature of 200 °C, oxygen partial pressure of 1.2 MPa, liquid–solid ratio of 10 mL/g, sodium lignosulfonate addition of 0.5 pct mass of raw material, leaching time of 120 minutes, and stirring speed of 400 r/min, copper leaching rate can reach 99.86 pct. At this time, the iron content of leaching solution is only 4.3 g/L; Chalcopyrite ($CuFeS_2$), porphyrite (Cu_5FeS_4), pyrite (FeS_2), galena (PbS), and other mineral phases can completely react in the system to form corresponding metal sulfate, and Fe^{3+} is converted to hematite by directed hydrolysis, thus inhibiting the generation of dangerous solid waste such as lead jarosite.

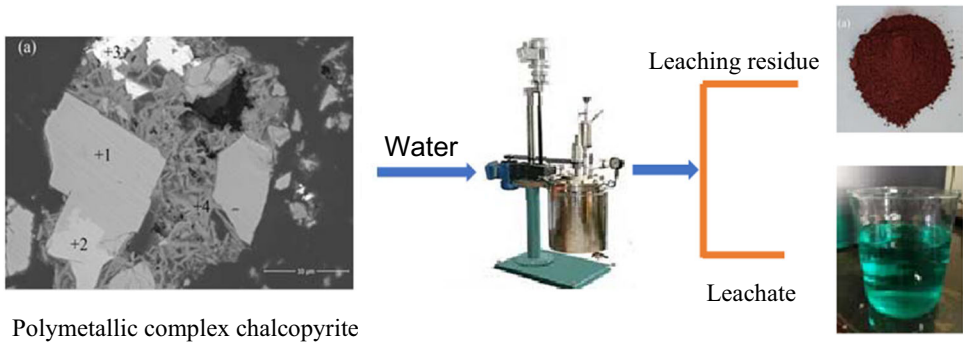

https://doi.org/10.1007/s11663-023-02858-6

I. INTRODUCTION

WORLDWIDE demand for copper is increasing rapidly and will continue until 2050.[1,2] Copper mineral resources consist mainly of sulfide minerals, among which chalcopyrite ($CuFeS_2$) is the sulfide form mineral with the widest distribution and largest reserves,[3] accounting for about 70 pct of the total copper resources.[4,5] However, with the production and consumption of mineral resources, the grade of copper ore is falling now, and its composition is more complex, which has paragenetic or associated relation with lead, iron, zinc, and other elements. Moreover, as the reason

JIAJUN XI, GUANGXIONG JI, YALONG LIAO, QINGFENG LIU, and YUE WU are with the Faculty of Metallurgical and Energy Engineering, Kunming University of Science and Technology, No. 253 Xuefu Road, Kunming 650093, Yunnan, P.R. China. Contact e-mail: liaoylsy@163.com

Jiajun Xi and Guangxiong Ji have contributed to the work equally and should be regarded as co-first authors.

Manuscript submitted December 15, 2022; accepted June 30, 2023. Article published online July 21, 2023.

that the fine granularity and the mosaic distribution of mineral phases composing copper ore, it is difficult to get the corresponding metal concentrates even ore dressing was performed, resulting lots production of polymetallic complex chalcopyrite with low content of copper, zinc, but high lead and iron content.[6–8]

At present, there is no suitable technology for efficient and clean extraction and utilization of polymetallic complex chalcopyrite. While traditional pyrometallurgical process is conducted to treat polymetallic complex chalcopyrite as the raw material either for copper smelting or for lead smelting, it will cause the loss of valuable metals such as copper and lead, high energy consumption, and environmental pollution.[9–11] In order to solve these various problems existing in the treatment of polymetallic complex chalcopyrite by traditional pyrometallurgical process, hydrometallurgical extraction processes with good environmental compatibility have gradually become a research hotspot.[12] Among of them microbial leaching,[13–15] high ferric salt leaching,[16,17] chlorine salt leaching,[18,19] organic acid leaching,[20] and *so on* are widely studied. However, in the leaching process, passivation layer composed of elemental sulfur,[21] copper and/or ferrous polysulfide,[17] jarosite,[22] and other products is easy to form on the surface of the reactants, which hinders copper leaching. Oxygen pressure leaching technology for chalcopyrite treatment can improve the leaching efficiency of copper,[23–25] but copper and iron co-leaching in the leaching process leads to the problem of high iron content in the leaching solution.[26] In addition, when the content of lead in minerals is high, lead jarosite residue and other dangerous solid wastes will be produced in the oxygen pressure acid leaching process, causing environmental pollution and harm to human body.[27,28]

This study aims at resolving difficult problems while oxygen pressure acid leaching is performed on polymetallic complex chalcopyrite with high lead and iron content, such as co-leaching of copper and iron, hazardous solid wastes like iron vitriol easily produced in residue, and etc. The methodology proposed in the present work is hydrothermal leaching under oxygen pressure without acid to efficient leach copper and synchronous to implement phase structure directional transformation for output harmless hematite residue which can easy be used. During the hydrothermal leaching, sodium lignosulfonate as a surfactant that can disperse molten sulfur located on the surface of raw material is needed.[29] In addition, as the reason that zinc in the form of sphalerite contained in the raw material is to be completely leached under the conditions involved in the present work, therefore the leaching of zinc is not listed in this paper. Moreover, lead in the form of galena in the raw material is transformed to lead sulfate which only deposits in the leaching residue, the leaching performance of lead is not mentioned in this work, and the more attention need to be paid is its occurrence in the residue. What's more, the separation and extraction of copper and zinc from leachate can be easily performed by traditional methodology like solvent extraction, ion exchange, and etc., how to treat the leachate obtained in this study is not involved.

II. EXPERIMENTAL

A. *Main Equipment*

The hydrothermal leaching under oxygen pressure experiments was carried out in an autoclave with a volume of 2 L (GSH-2, Weihai Chemical Machinery Co. Ltd, China), which equipped with sampling system, heating and cooling system with the working temperature range of 0 °C to 250 °C, as well as stirring system at the speed range of 0 to 800 r/min. In addition, the material of autoclave body was zirconium, and the schematic diagram of the device is shown in Figure 1.

B. *Testing and Characterizing Method*

X-ray diffraction (XRD, PANalytical Xpert3 powder diffractometer, Netherlands), scanning electron microscopy, and energy-dispersive spectroscopy (SEM-EDS, JSM-6360, Japan) were used to characterize the mineral phase structure and morphology of raw materials and leaching residues. The chemical elements of raw materials and leaching residues were quantitatively analyzed by inductively coupled atomic emission spectrometer (ICP-AES, Pekin-Elmer Optima-5300DV) and carbon sulfur analyzer (Eltra CS2000, German). The content of copper in leaching solution was determined by ultraviolet and visible spectrophotometer, and the content of iron was determined by potassium dichromate titration.

The leaching rate index reflecting the leaching effect of copper and iron is calculated according to Formula [1]. All the data listed in the present work are the average of three parallel experiments under the same conditions.

$$\eta_x = \frac{w_{xi}}{w_{xo}} \times 100\,\text{pct}, \qquad [1]$$

where η_x is the leaching rate of copper and iron, W_{xi} is the mass of copper and iron in the leaching solution (g), and W_{xo} is the mass of copper and iron in the raw materials used for leaching (g).

C. *Raw Materials*

Polymetallic complex chalcopyrite was obtained from an ore dressing plant in Yunnan province, China. Raw material with particle size less than 45 μm used in the present work was achieved by wet ball milling, filtration and drying. The contents of main elements in the raw material were determined by ICP-AES, and the results are shown in Table I. From Table I, it is known that sulfur, iron, copper, and lead are the main elements constituting of the raw material, and these four elements in total accounted for more than 80 pct (mass fraction) of the material; the content of most valuable metals like copper and zinc content is low, while the content of impurity metals like lead and iron is high, indicating it

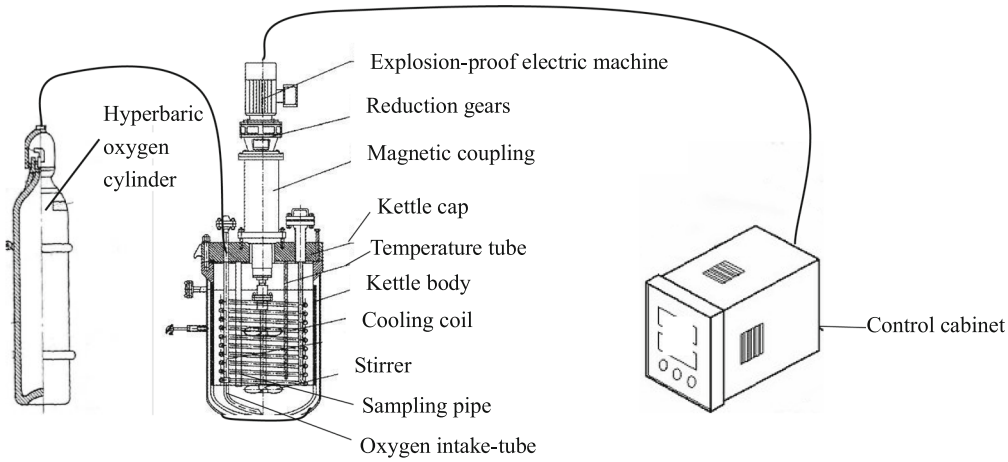

Fig. 1—Schematic diagram of experimental device.

Table I. The Main Element Content of Raw Materials (Mass Fraction Pct)

Cu	Fe	Pb	Zn	S	SiO_2	Al_2O_3	CaO	MgO
11.10	28.10	8.88	2.97	34.95	1.86	0.5	0.38	0.43

belongs to low-grade polymetallic complex sulfide copper. The content of copper (11.10 pct) in it is far lower than that the requirement of raw material grade (containing 20 to 30 pct copper) for pyrometallurgical copper smelting, so this kind of resources belong to the refractory resources that cannot be utilized by traditional pyrometallurgical smelting.[30] XRD was carried out on the raw material to analyze its phase composition, and the obtained result is illustrated in Figure 2 which shows that the crystallized phase mainly includes chalcopyrite ($CuFeS_2$), porphyrite (Cu_5FeS_4), pyrite (FeS_2), galena (PbS), sphalerite (ZnS), and quartz (SiO_2).

D. *Procedure of Hydrothermal Leaching Under Oxygen Pressure*

Hundred grams of raw material and 0.5 g of sodium lignosulfonate as a surfactant for getting high leaching rate[31] were weighed and mixed evenly and put into the autoclave, then a certain volume of distilled water according to the preset liquid–solid ratio was added before sealing the autoclave, followed by stirring and heating. When the temperature of the system reaches the specified temperature, oxygen with the specified pressure is passed in for leaching reaction. After the reaction complementation, the oxygen valve of the heating device was closed and the cooling system was turned on to reduce the temperature of the reaction system to room temperature, followed by turning off the stirring and relieving the remained pressure, turning on the autoclave to pour out the leaching pulp. The leaching pulp was filtered and washed on the vacuum filter extraction device to collect the filtrate and wash liquid, and the filter cake obtained was put in an oven to be dried at 110 °C for 2 hours.

III. RESULTS AND DISCUSSION

A. *Effects of Sulfuric Acid*

Changing the concentration of sulfuric acid in the initial leaching solution (0, 10, 20, 30, 40, 50 g/L) for studying the influence of initial acid concentration of leaching agent on leaching rate of copper and iron in leaching process was performed, under the conditions of leaching temperature of 200 °C, liquid–solid ratio of 10 mL/g, partial pressure of oxygen of 1.2 MPa, leaching time of 120 minutes, and stirring speed of 400 r/min, and the results obtained are shown in Figure 3.

It can be found from Figure 3 that the initial sulfuric acid concentration within the range of 0 to 50 g/L, the leaching rate of copper does not change much, reaching more than 99 pct. However, the leaching rate of iron increases with the increase of initial sulfuric acid concentration. This is because that in this acidity range mentioned above, Fe^{3+} is mainly precipitated in the form of hematite, which is inhibited by the increase of acidity. However, when the initial acidity is greater than 20 g/L, the iron leaching rate gradually decreases due to the existence of $PbSO_4$ in the system resulting from the dissociation of galena, and the increase of acidity changes the hydrolysis reaction of ferric iron from hematite iron precipitation to basic ferric sulfate and jarosite-coordinated iron precipitation.[32–34]

XRD characterization was carried out on the leaching residues obtained with different initial sulfuric acid concentrations, and the influence of initial acidity on the phase composition of the leaching residues was analyzed. The transformation of the mineral phase of leaching residue with initial acidity is shown in Figure 4. As can be seen from Figure 4 that the lead jarosite phase always exists in the leaching residue with the increase of initial

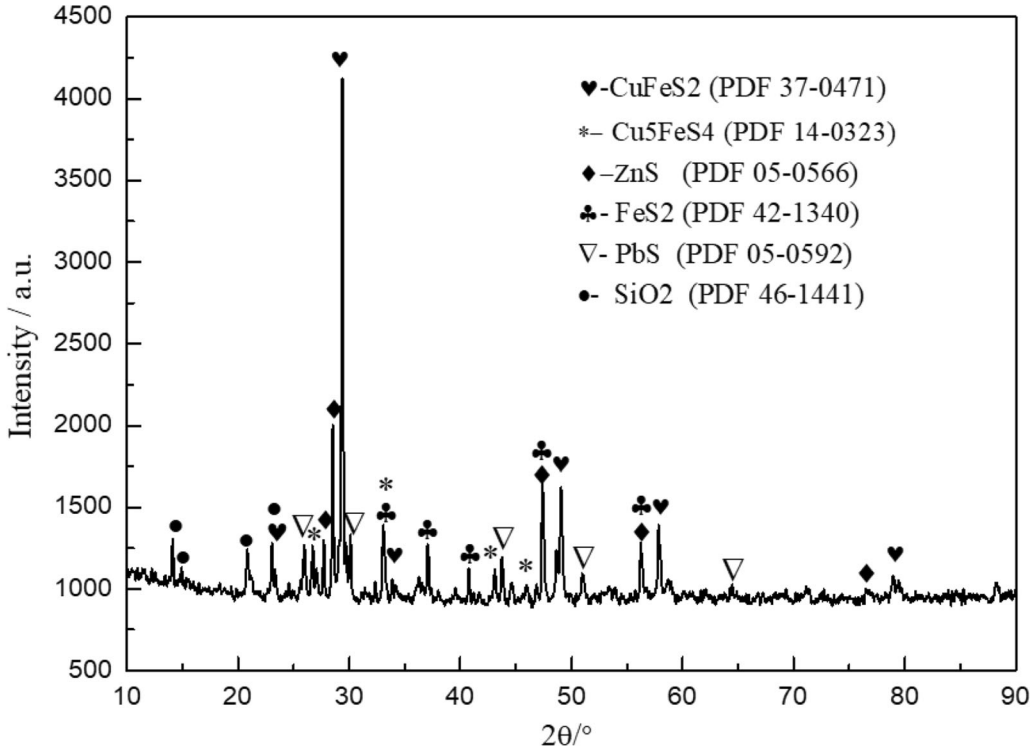

Fig. 2—XRD pattern of raw materials.

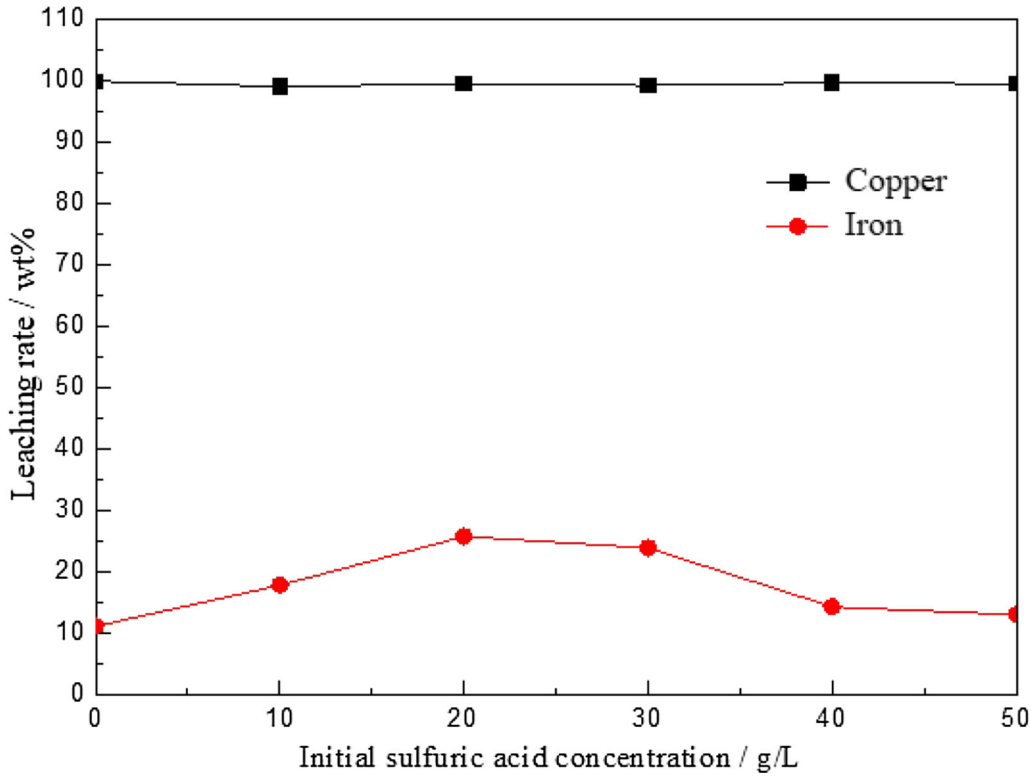

Fig. 3—The effects of initial acidity on the leaching rate of copper and iron.

sulfuric acid concentration and that there is an obvious $PbSO_4$ phase peak in the leaching residue when the initial sulfuric acid concentration is 0 g/L, but which gradually disappears with the increase of the initial sulfuric acid concentration, indicating that the increase of the initial sulfuric acid concentration will cause the transformation

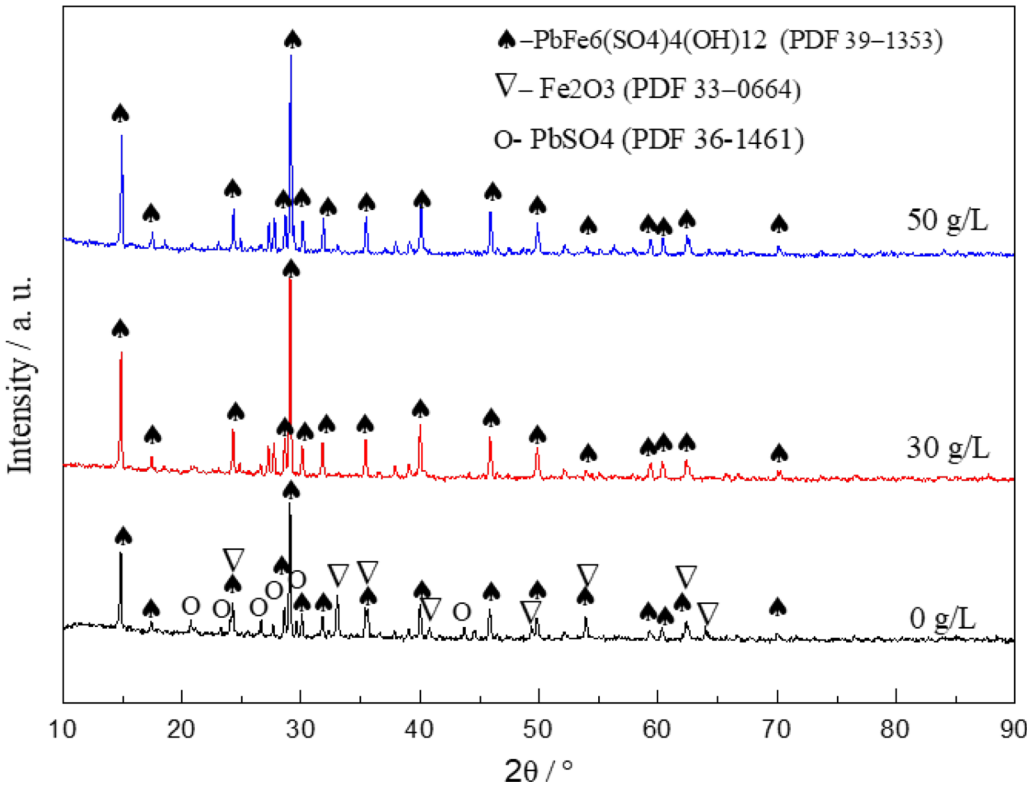

Fig. 4—XRD patterns of leaching residues under different initial acidity.

of $PbSO_4$ into lead jarosite in the system. In addition, when the initial sulfuric acid concentration is 0 g/L, there is an obvious Fe_2O_3 peak in the leaching residue, which gradually disappears with the increase of the initial sulfuric acid concentration when the initial sulfuric acid concentration is greater than 30 g/L, which indicates that the increase of acidity will change the precipitation mode of Fe^{3+} in the system. As a result, the mineral phase of leaching residue transforms from hematite to lead jarosite.[35–38] The chemical reaction equation of residue phase transformation is shown in Eqs. [2] and [3].

$$2Fe^{3+} + 3H_2O = Fe_2O_3 + 6H^+ \quad [2]$$

$$6Fe^{3+} + 3SO_4{}^{2-} + 12H_2O + PbSO_4 = PbFe_6(SO_4)_4(OH)_{12} + 12H^+ \quad [3]$$

With the difference of initial sulfuric acid concentration, the color of leaching residue changes from reddish brown representing hematite to yellowish brown (color of lead jarosite),[39–41] which can be found in Figure 5.

The obtained leaching residue was characterized by SEM-EDS, and the influence of the initial sulfuric acid concentration on the morphology and structure of the leaching residue was analyzed. The morphology and structure of the leaching residue varied with the initial acidity are shown in Figure 6 (0 g/L) and Figure 7 (50 g/L), as well as the chemical content of them is listed in Table II which indicate 90.5 and 41.5 pct of the iron in the leaching residue are existed with the form of Fe_2O_3, respectively.

It can also be seen from Figure 6 that when the initial sulfuric acid concentration is 0 g/L, the leaching residue presents a loose porous structure, which mainly consists of Fe_2O_3, with a small amount of lead jarosite with tetrahedral structure and basic ferric sulfate with rod-like structure wrapped. According to Figure 7, when the initial sulfuric acid concentration is 50 g/L, the leaching residue is mainly composed of tetrahedral lead jarosite and a small amount of basic ferric sulfate with rod-like structure. Compared with the initial sulfuric acid concentration of 0 g/L, it is found that the leaching residue has fine particle size, smooth surface, compact structure, and no obvious wrapping and distribution relationship.

In conclusion, the initial sulfuric acid concentration of 0 g/L is the best choice. Under this condition, more than 99 pct of the copper in the raw material is dissolved into the leaching solution, and about 90.5 pct of the iron is converted into hematite contained in the leaching residue, realizing the purpose of hydrothermal leaching of copper without sulfuric acid in the initial leaching solution. This process proposed in the present work can achieve efficient leaching of copper and directional transformation of iron into hematite in leaching residue, not only reducing the cost for disposal polymetallic complex chalcopyrite but also reducing the requirement of anti-corrosion performance of equipment in leaching process.

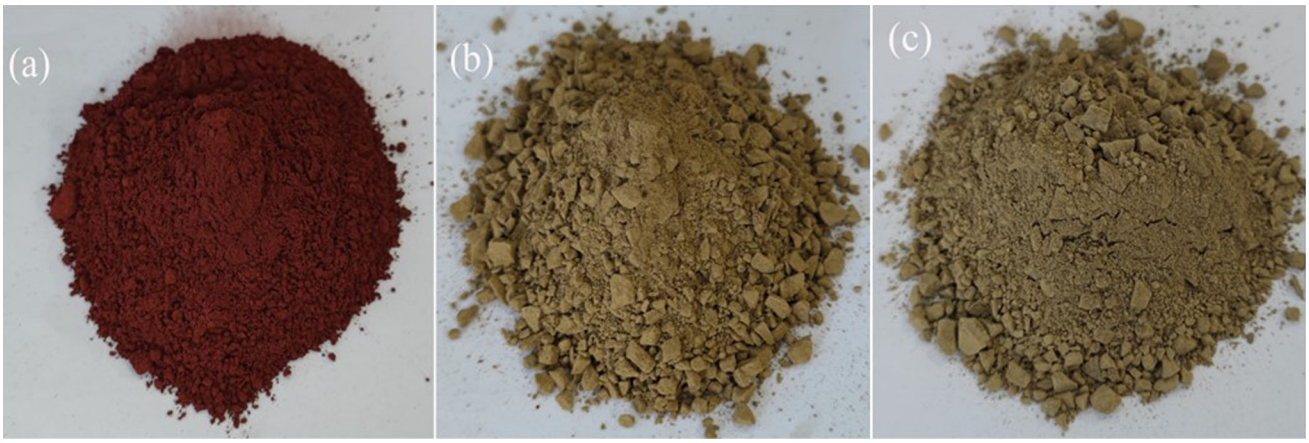

Fig. 5—Effect of initial sulfuric acid concentration (*a*: 0 g/L, *b*: 30 g/L, *c*: 50 g/L) on the color of leaching residue (Color figure online).

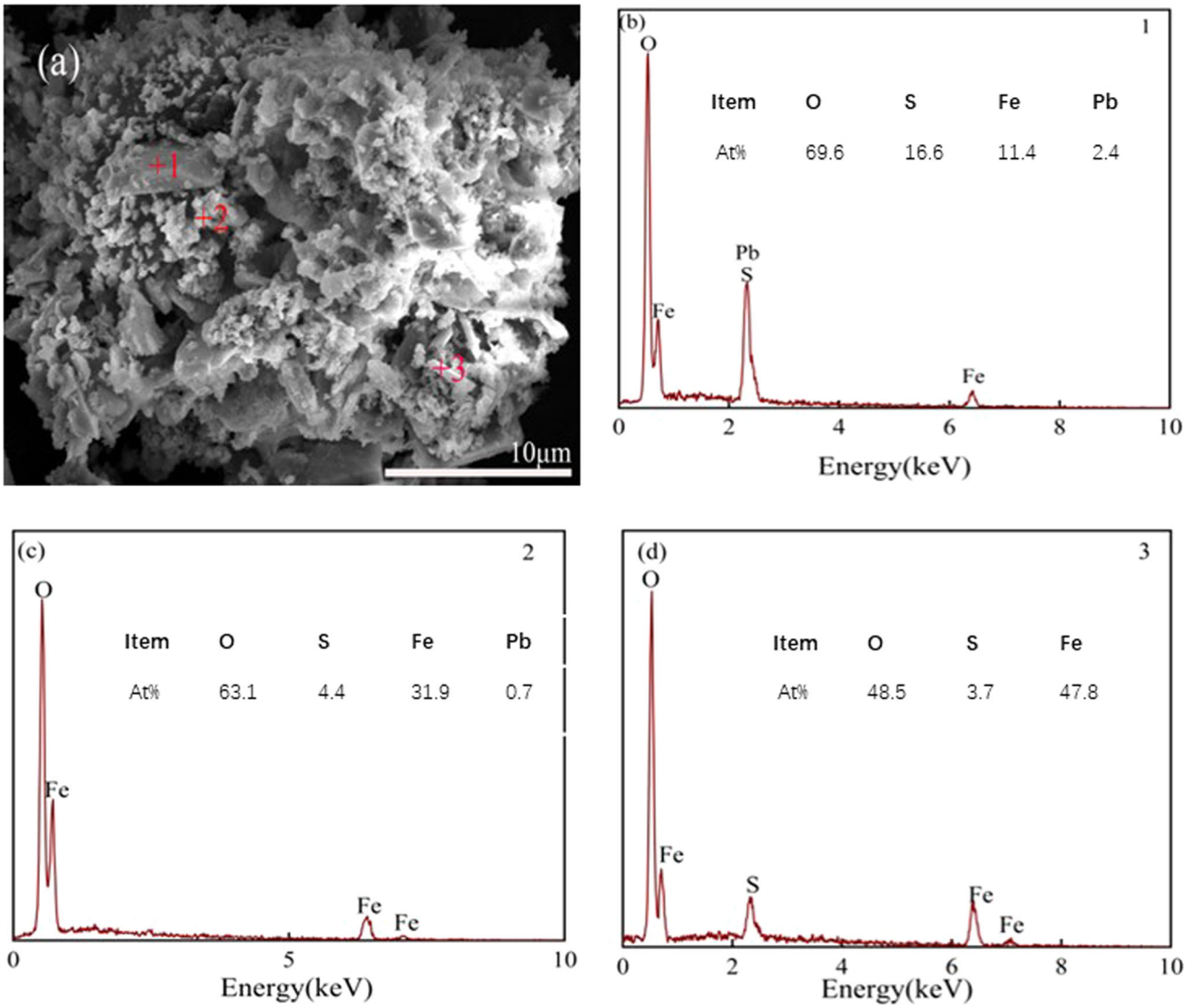

Fig. 6—SEM image (*a*) and EDS spectrum (*b* through *d*) of leaching residue obtained with the initial acidity of 0 g/L.

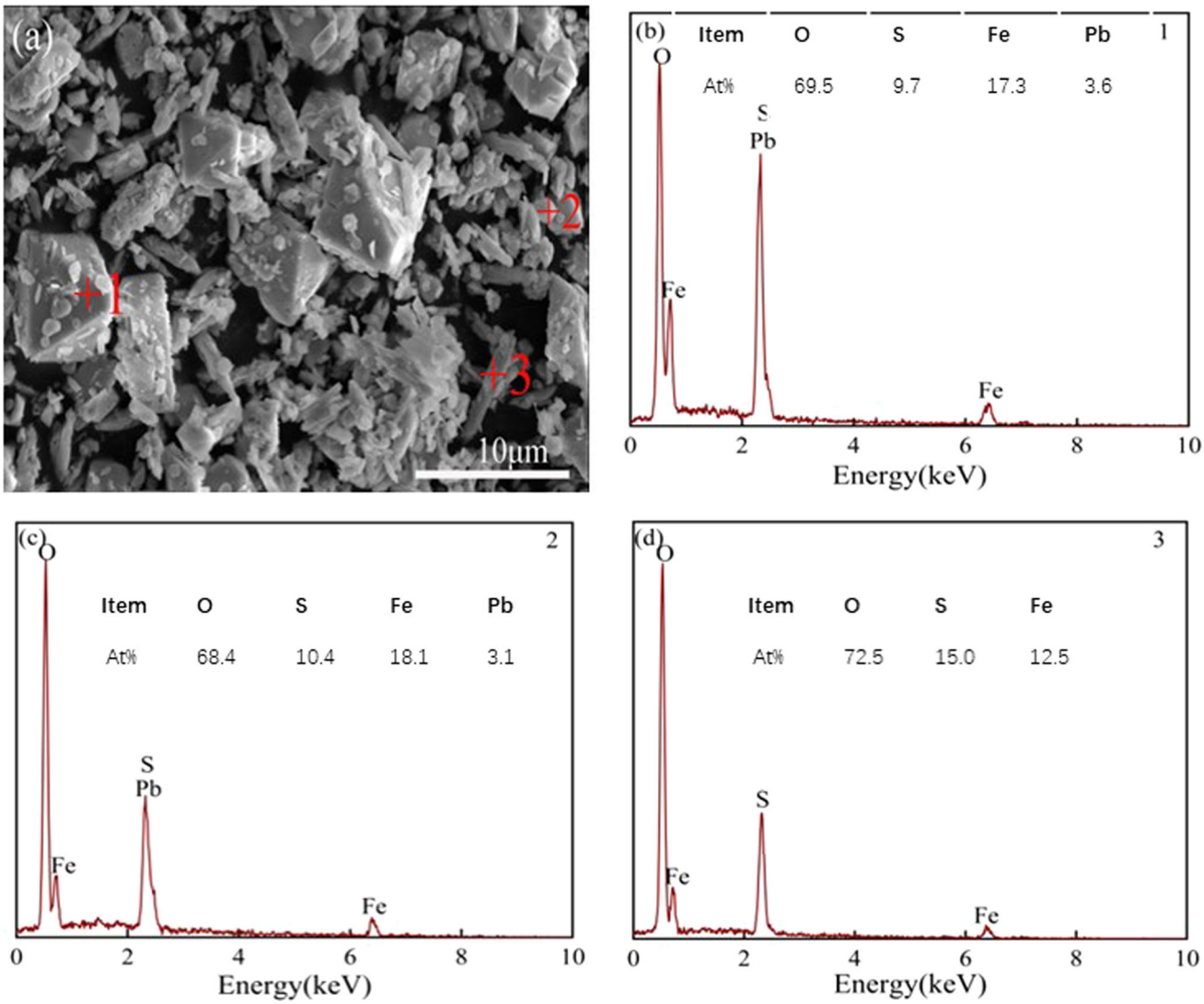

Fig. 7—SEM image (*a*) and EDS spectrum (*b* through *d*) of leaching residue obtained with the initial acidity of 50 g/L.

Table II. The Chemical Content of Leaching Residues at Different Initial Acidity

		Content, Wt Pct								
Item (g/L)	Mass, g	Cu	TFe	Fe_2O_3	Pb	Zn	S	SiO_2	CaO	MgO
0	60.88	0.025	41.00	53.01	14.57	0.06	3.29	3.03	0.60	0.02
50	72.80	0.082	33.52	19.86	12.06	0.04	7.63	2.50	0.51	0.01

B. *Effects of Reaction Temperature*

Under the experimental conditions of initial sulfuric acid concentration of 0 g/L, liquid–solid ratio of 10 mL/g, oxygen partial pressure of 1.2 MPa, leaching time of 120 minutes, sodium lignosulfonate addition of 0.5 pct mass of raw material, and stirring speed of 400 r/min, the influence of reaction temperature on leaching behavior of copper and iron from raw material by hydrothermal leaching under oxygen pressure was studied. Five groups of experiments were designed at reaction temperature of 140 °C, 160 °C, 180 °C, 200 °C, and 220 °C, respectively. The results on the influence of reaction temperature on the leaching rate of copper and iron by hydrothermal leaching under oxygen pressure are shown in Figure 8.

Figure 8 shows that the copper leaching rate increases with the increase of temperature when the reaction temperature of the system increases from 140 °C to 220 °C and that it reaches over 99 pct while the temperature reaches 200 °C and nearly remains unchanged even though the temperature continuously increase. The results show that high temperature is

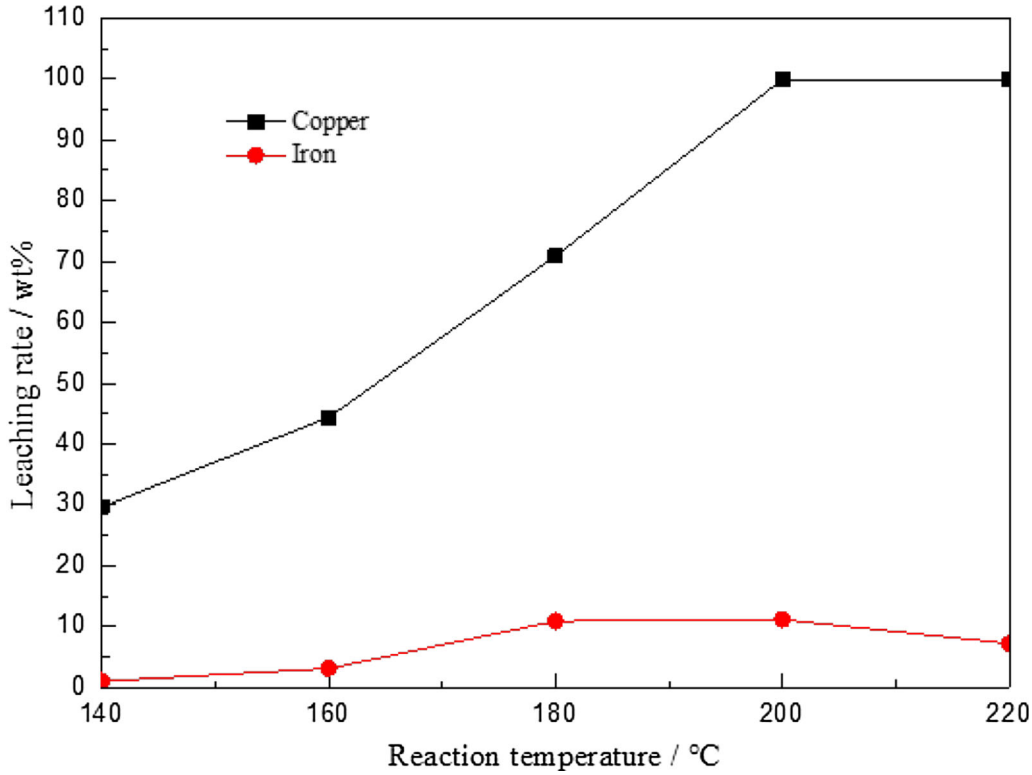

Fig. 8—The effects of temperature on the leaching rate of copper and iron.

favorable for mineral dissociation and copper completely enters the leaching solution. On the premise of complete leaching of copper, the iron leaching rate is 11.17 pct at 200 °C; however, it is reduced by 3.95 pct at 220 °C, indicating that high temperature is favorable for Fe^{3+} hydrolysis.[42] Although the leaching rate of iron at 200 °C is higher than that at 220 °C, the leaching rate of copper is basically unchanged while the temperature increases by 220 °C from 200 °C, and the saturated vapor pressure of the leaching system increases sharply after the reaction temperature is higher than 200 °C, which will make the energy consumption of the reaction system increased, and the requirements for the equipment material to withstand higher pressure, so it is not advocated to make the leaching reaction occurred at 220 °C.

The change of phase composition of leaching residue at different reaction temperatures is shown in Figure 9. It can be seen from Figure 9 that with the increase of reaction temperature, the phase peaks of lead jarosite and lead sulfate in the leaching residue basically do not change, but the intensity of Fe_2O_3 phase peak is obviously strengthened with the increase of reaction temperature, indicating that the increase of reaction temperature is conducive to the precipitation of iron in the system in the form of hematite and the transformation of leaching residue to hematite.[43,44]

The leaching residue at 180 °C was characterized by SEM-EDS, and the influence of reaction temperature on the morphology and structure of the leaching residue was analyzed. The morphology and structure of the leaching residue at 180 °C and 200 °C are shown in Figures 10 and 6, respectively. In addition, the chemical element content of the leaching residue obtained at 180 °C also listed in Table III, which also means part of chalcopyrite in the raw material is not completely dissolved.

Compared with the leaching residue at 200 °C, the particle size of the leaching residue at 180 °C is smaller, and there are unwrapped lead jarosite, tetrahedral structure, and massive structure of lead sulfate. In addition, hematite is wrapped on the surface of unreacted minerals in the form of fine particles at 180 °C. Considering the selective leaching rate and energy consumption of copper and iron, the optimum reaction temperature is 200 °C. Under this condition, more than 99 pct of the copper in mineral transfers into the leaching solution, the content of iron in the leaching solution is only 4.3g /L, and 90.5 pct of the iron contained in the leaching residue is in the form of hematite.

C. *Effects of Oxygen Partial Pressure*

Under the experimental conditions of initial sulfuric acid concentration of 0 g/L, reaction temperature of 200 °C, liquid–solid ratio of 10 mL/g, leaching time of 120 minutes, sodium lignosulfonate addition of 0.5 pct mass of raw material, and stirring speed of 400 r/min, the influence of oxygen partial pressure on hydrothermal leaching under oxygen pressure was studied. Five groups of experiments were designed with oxygen partial

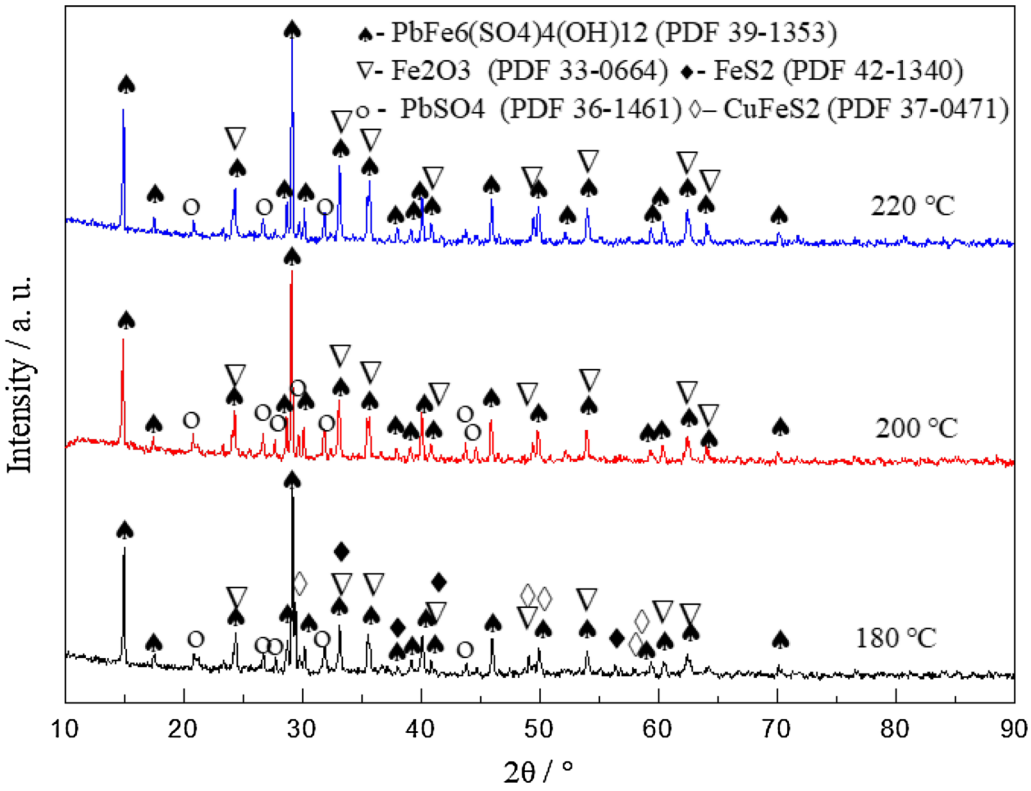

Fig. 9—XRD patterns of leaching residues at different reaction temperatures.

pressures at 0.6, 0.8, 1.0, 1.2, and 1.4 MPa, respectively. The influence of oxygen partial pressures on the leaching is shown in Figure 11.

It can be seen from Figure 11 that when the oxygen partial pressure of the system is increased from 0.6 to 1.4 MPa, the leaching rate of copper increases with the increase of oxygen partial pressure and gradually tends to be gentle. This is because oxygen is needed not only for dissolution of sulfide minerals in the raw material, but also for oxidation of Fe^{2+}, and the higher partial pressure of oxygen helps to improve the concentration of dissolved oxygen in the leaching system, so that the oxidation atmosphere of the system can be maintained at a higher level, thus promoting the dissociation of the mineral phase in raw material and improving the leaching rate of copper. While the oxygen partial pressure is lower than 0.8 MPa, the iron leaching rate increases with the increase of oxygen partial pressure, which is because the increase of oxygen partial pressure promotes the dissociation of mineral phase and releases more iron in the leaching solution as Fe^{2+}. After it exceeds 0.8 MPa, due to the further increase of oxygen partial pressure, Fe^{2+} ions in the system can be oxidized to Fe^{3+} and then hydrolysis reaction of $Fe_2(SO_4)_3$ to form Fe_2O_3 occurs, thus reducing the iron leaching rate.

For analyzing the influence of oxygen partial pressure on the phase composition of leaching residue, the typical leaching residue under corresponding conditions was characterized by XRD. The obtained results is shown in Figure 12.

It can be seen from Figure 12 that the peak intensity of lead jarosite in the XRD pattern of the leaching residue at 0.8 MPa is obviously low. Combined with the leaching rate of copper 61.47 pct under this experimental condition, it indicates that the mineral dissociation in the system under this partial oxygen pressure is not sufficient, thus inhibiting the transformation of iron into lead jarosite in the leaching system. When oxygen partial pressure is greater than 0.8 MPa, the peak of lead jarosite is more obvious, and the peak strength of Fe_2O_3 is obviously strengthened with the increase of oxygen partial pressure, indicating that higher oxygen partial pressure benefits not only to fully dissociate the mineral phase in raw material, but also to facilitate the transformation of iron to hematite in the leaching residue.

D. *Ratio of liquid to solid*

Under the experimental conditions of initial sulfuric acid concentration of 0 g/L, reaction temperature of 200 °C, partial pressure of oxygen of 1.2 MPa, leaching time of 120 minutes, addition of sodium lignosulfonate of 0.5 pct mass of raw materia,l and stirring speed of 400 r/min, the influence of liquid–solid ratio on the leaching of minerals in hydrothermal leaching under oxygen pressure was studied. Four groups of experiments with liquid–solid ratio at 6, 8, 10, and 12 mL/g were designed, and the results obtained are shown in Figure 13. Figure 13 shows that when the liquid–solid ratio of the leaching system is increased from 6 to 12 mL/g, the copper leaching rate basically remains unchanged.

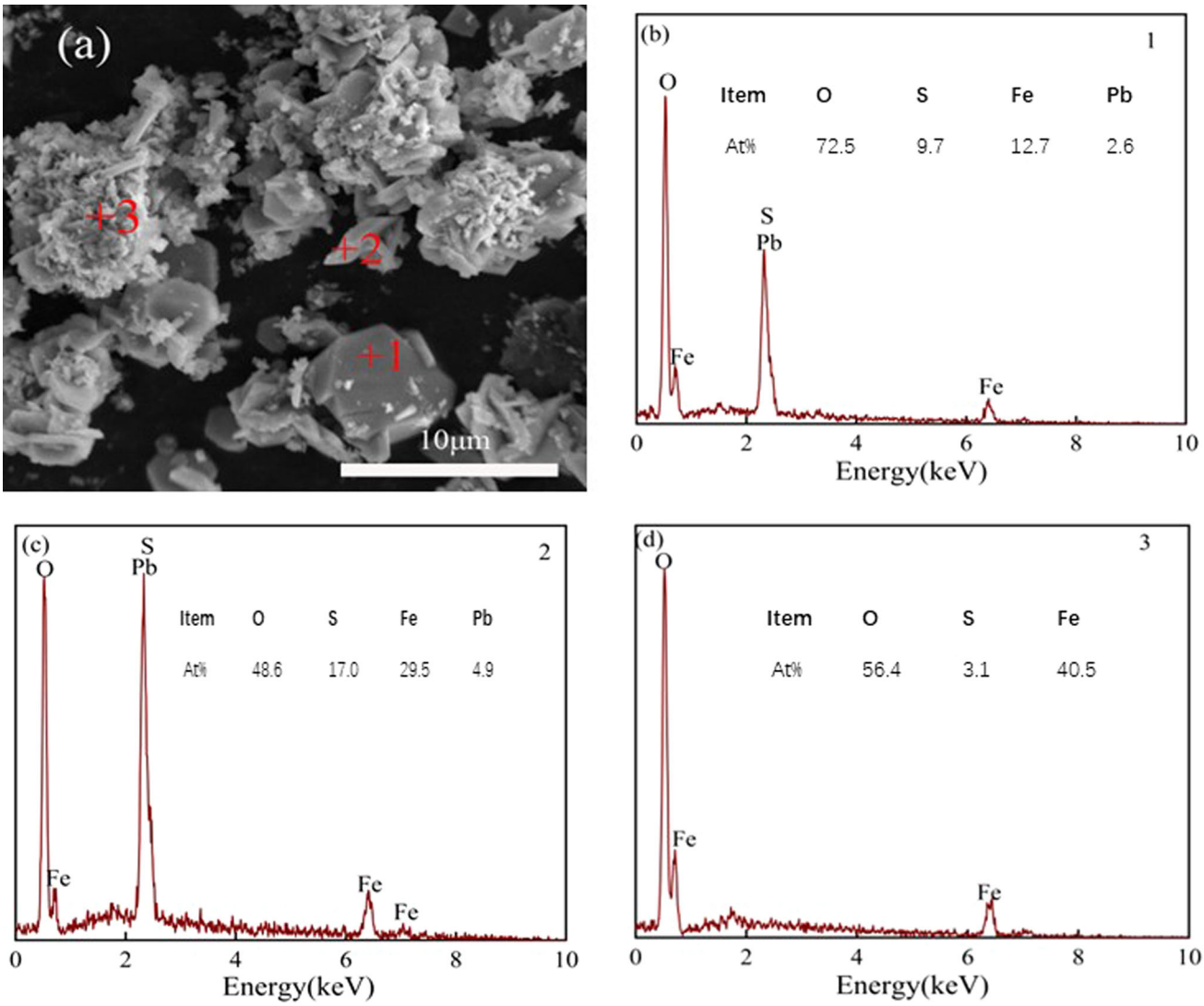

Fig. 10—SEM image (*a*) and EDS spectrum (*b* through *d*) of leaching residue of 180 °C.

However, when the liquid to solid ratio is 10 mL/g, the leaching rate of iron is the lowest; this could be accounted for by the reason that the low liquid to solid ratio leads to the high acid concentration in the system, which inhibits the hydrolysis of ferric ion in leaching solution and even leads to the redissolution of part of hematite contained in leaching residue. When the liquid–solid ratio increased to 12 mL/g from 10 mL/g, the iron leaching rate increased by about 20 pct. This is because the excessive liquid–solid ratio reduces the volume of gaseous phase in the reaction system, leading the oxygen quantity in atmosphere of the system and the dissociation rate of mineral in the raw material lower. In addition, Fe^{3+} is mainly transformed into Fe^{2+} retaining in the leaching solution while oxygen is insufficient, as shown in Eq. [4], and iron cannot be precipitated from leaching solution with the form of Fe_2O_3 as Eq. [2] mentioned above, leading to an increase in the iron leaching rate.[45,46] The results obtained show that the liquid–solid ratio of 10 mL/g is the best choice.

$$MeS + 2Fe^{3+} = Me^{2+} + 2Fe^{2+} + S^0 \qquad [4]$$

In Eq. [5], MeS represents the main sulfide phases in raw material, mainly chalcopyrite ($CuFeS_2$), porphyrite (Cu_5FeS_4), pyrite (FeS_2), galena (PbS), and sphalerite (ZnS)

E. *Effects of leaching time*

Under the experimental conditions of initial acidity of 0 g/L, reaction temperature of 200 °C, oxygen partial pressure of 1.2 MPa, liquid–solid ratio of 10 mL/g, addition of sodium lignosulfonate of 0.5 pct mass of raw material, and stirring speed of 400 r/min, the influence of

Table III. The Chemical Content of Leaching Residues at 180 °C

Item	Mass, g	Content, Wt Pct							
		Cu	Fe	Pb	Zn	S	SiO_2	CaO	MgO
180 °C	70.77	4.57	35.37	12.45	0.13	13.48	2.61	0.52	0.01

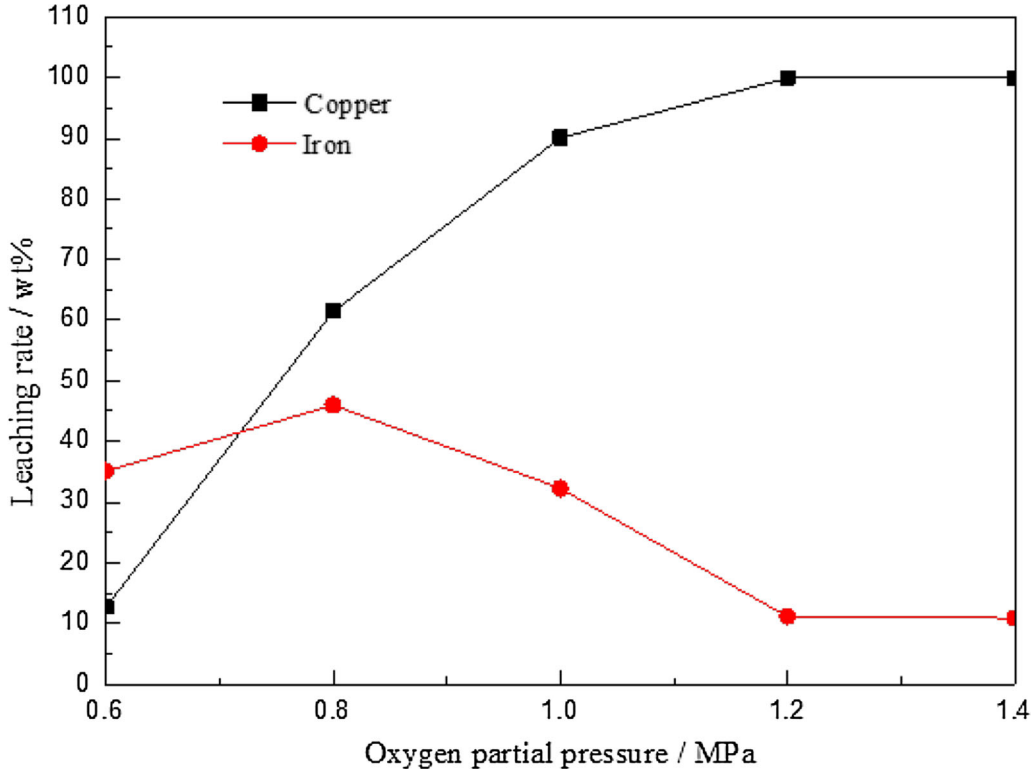

Fig. 11—Effects of oxygen partial pressure on the leaching rate of copper.

leaching time on leaching behavior of valuable metals in the raw material by hydrothermal leaching under oxygen pressure was studied. Five groups of experiments were designed with different leaching time at 30, 60, 90, 120, and 150 minutes, respectively. The influence of leaching time on the selective leaching rate of copper and iron by hydrothermal leaching under oxygen pressure is shown in Figure 14. With the increase of leaching time, copper leaching firstly increases and then tends to be stable. When leaching time is 120 minutes, copper leaching is almost complete. The leaching rate of iron increases first and then decreases with the increase of leaching time. The leaching rate reaches the lowest 8.51 pct at 150 minutes, but the decrease is not large compared with that at 120 minutes.

The representative leaching residue under corresponding conditions was characterized by XRD, and the influence of leaching time on the phase composition of leaching residue was analyzed. The results are shown in Figure 15.

It can be seen from Figure 15 that, compared with raw materials, galena and sphalerite have disappeared in the leaching residue after the reaction time of 30 minutes, but chalcopyrite and pyrite do not completely be dissolved. Chalcopyrite and pyrite have basically disappeared after the reaction time of 90 minutes, indicating that the leaching reaction of galena and sphalerite is easier than that of chalcopyrite and pyrite. In addition, with the increase of leaching time, phases such as lead sulfate, hematite, and lead jarosite gradually appear in the leaching residue. The results show that the formation time of lead jarosite mainly occurs in the period of 60 to 90 minutes, and the phase composition in the leaching residue basically does not change significantly after 90 minutes. Chemical reactions as shown in Eqs. [5] through [9] mainly occur when major mineral phases are dissociated during the process of hydrothermal leaching under oxygen pressure atmospheric.[47]

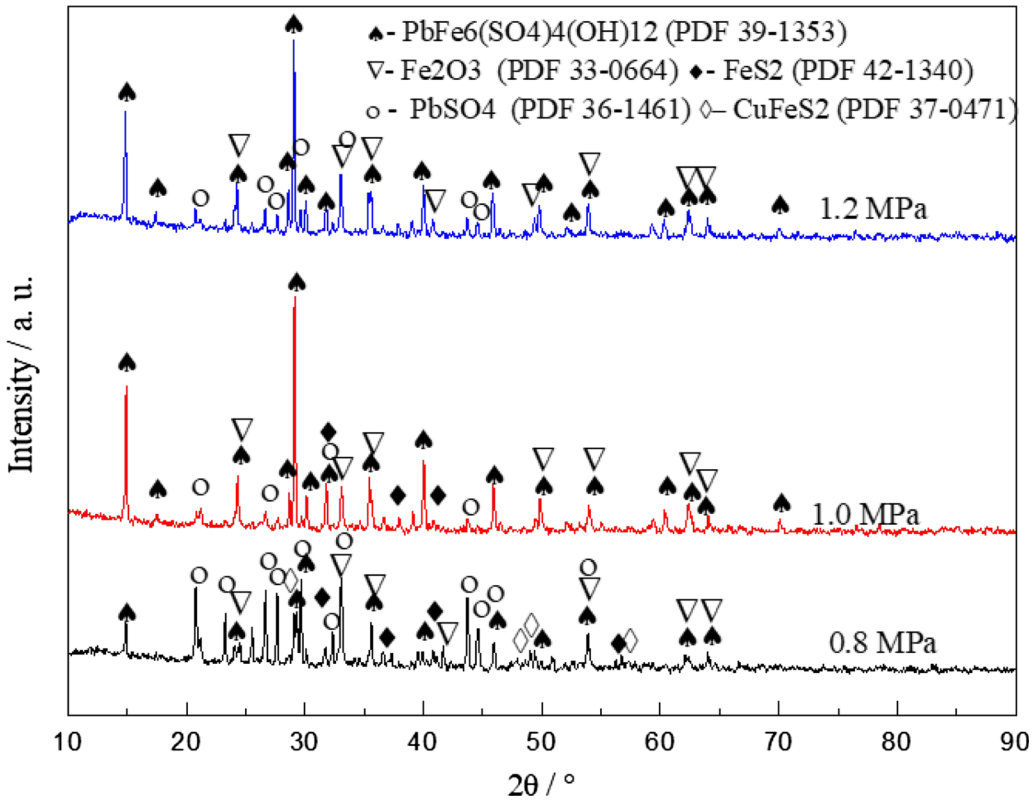

Fig. 12—XRD patterns of leaching residues under different oxygen partial pressures.

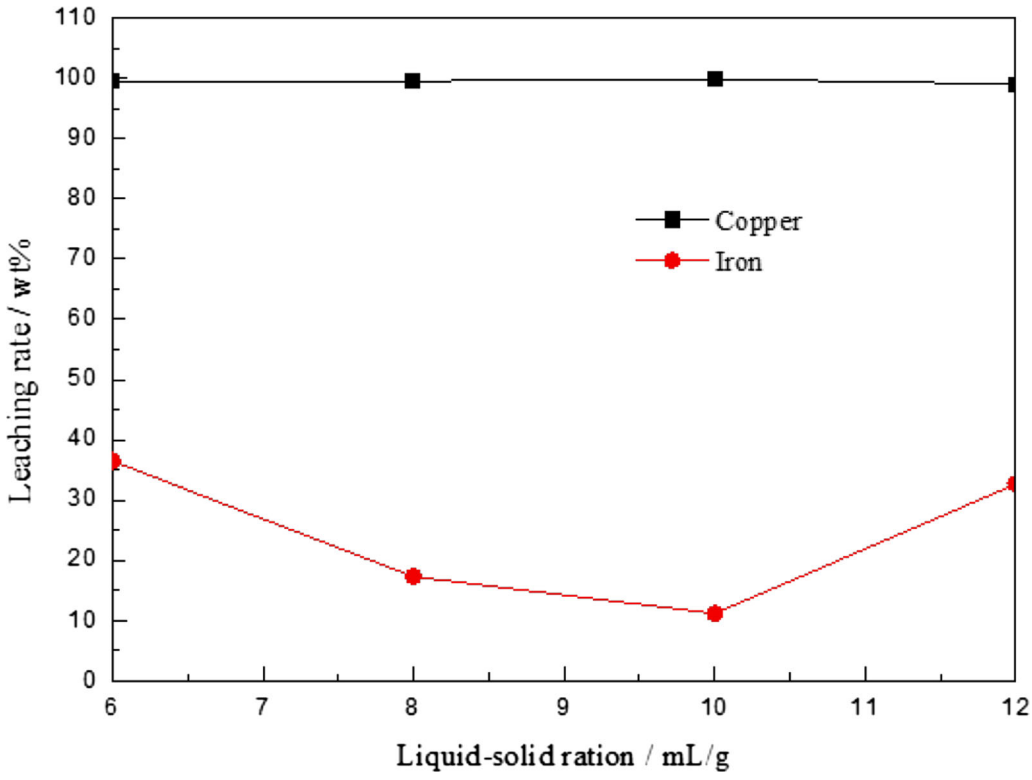

Fig. 13—The effects of liquid–solid ratio on the leaching rate of copper and iron.

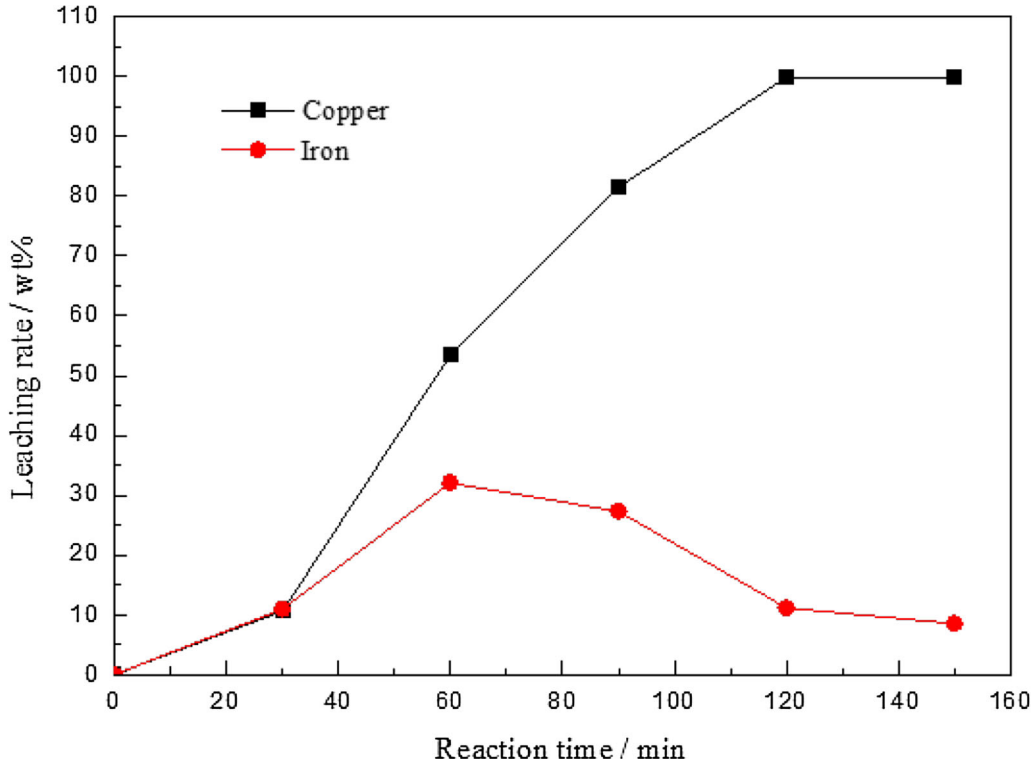

Fig. 14—The effects of leaching time on the leaching rate of copper and iron.

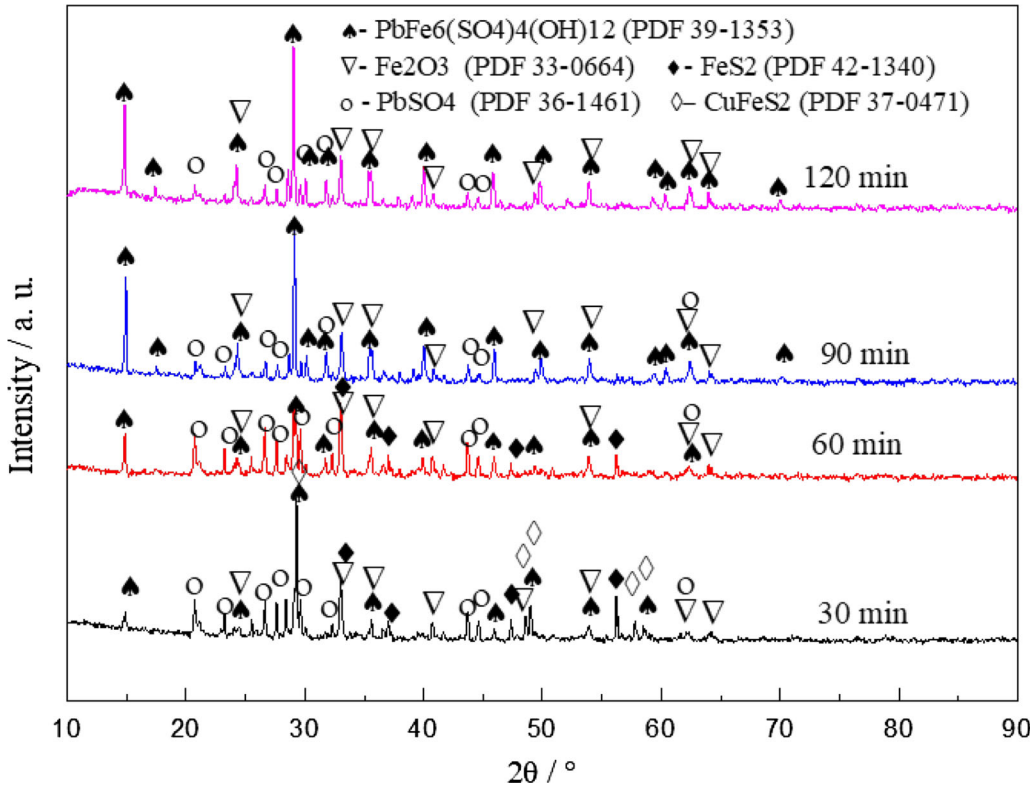

Fig. 15—XRD patterns of leaching residues under different leaching time.

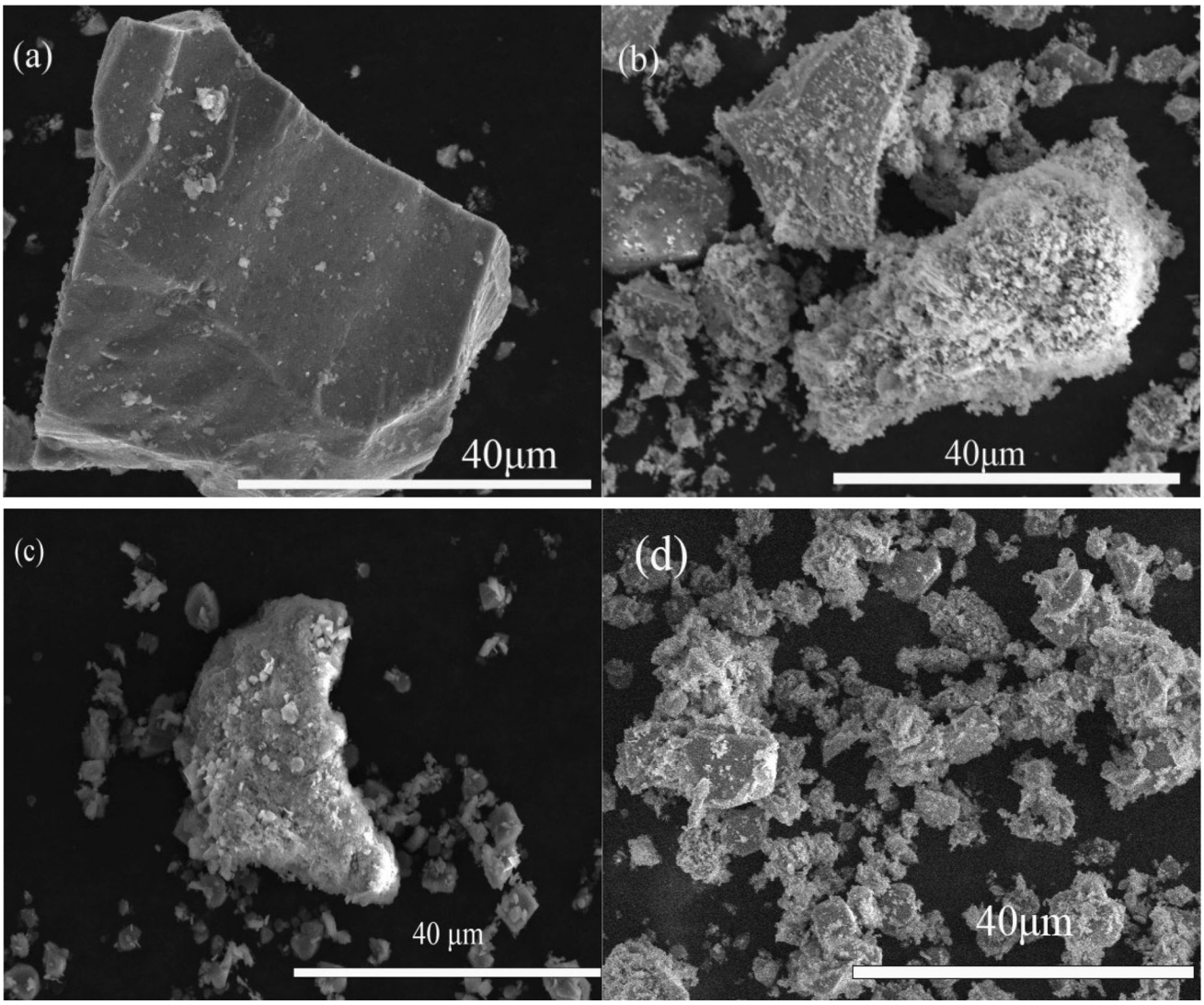

Fig. 16—SEM images of leaching residues at different leaching times (*a*: raw material; *b* 30 min; *c* 60min; *d* 90 min).

$$2PbS + 4H^+ + 2SO_4^{2-} + O_2 = 2PbSO_4 + 2S^0 + 2H_2O \quad [5]$$

$$2FeS_2 + 4H^+ + O_2 = 2Fe^{2+} + 4S^0 + 2H_2O \quad [6]$$

$$CuFeS_2 + 4H^+ + O_2 = Cu^{2+} + Fe^{2+} + 2S^0 + 2H_2O \quad [7]$$

$$2Fe^{2+} + 2H^+ + 0.5O_2 = 2Fe^{3+} + H_2O \quad [8]$$

$$2S^0 + 2H_2O + 3O_2 = 4H^+ + 2SO_4{}^{2-} \quad [9]$$

The leaching residue under different reaction time was characterized by SEM, and the influence of leaching time on the morphology of leaching residue was analyzed, the obtained result can be found in Figure 16. As can be seen from Figure 16, the surface of raw materials is smooth and compact. With the increase of reaction time, the mineral gradually dissociates, the particle size becomes smaller, and the products are wrapped on the mineral surface, and the surface becomes rough.

IV. CONCLUSION

The main minerals in polymetallic complex chalcopyrite are chalcopyrite ($CuFeS_2$), porphyrite (Cu_5FeS_4), pyrite (FeS_2), galena (PbS), sphalerite (ZnS), and quartz (SiO_2). Hydrothermal leaching under oxygen pressure without sulfuric acid in the initial leaching solution can directly extract copper from polymetallic complex

chalcopyrite and precipitate iron in the form of hematite in the leaching residue, thus achieving a highly selective separation of copper from iron. Under the experimental conditions of initial sulfuric acid concentration of 0 g/L, reaction temperature of 200 °C, oxygen partial pressure of 1.2 MPa, liquid–solid ratio of 10 mL/g, addition of sodium lignosulfonate of 0.5 pct mass of raw material, leaching time of 120 minutes, stirring speed of 400 r/min, the copper leaching rate can reach 99.86 pct, but the leaching rate of iron was only 11.17 pct. Compared with other factors, reaction temperature, oxygen partial pressure, and leaching time have a greater influence on the selective leaching rate of copper and iron in hydrothermal leaching process under oxygen pressure and are the key control factors to achieve high selective leaching and separation of copper and iron.

Hydrothermal leaching under oxygen pressure for disposal of polymetallic complex chalcopyrite resources can achieve efficient selective leaching of copper and iron, and directional control of phase composition and structure of leaching residue, effectively reduce the generation of dangerous solid wastes such as jarosite. Initial sulfuric acid concentration, reaction temperature, and oxygen partial pressure are the key factors for directional control of the phase transformation of leaching residue. Lower initial sulfuric acid concentration, higher reaction temperature, and oxygen partial pressure are favorable for the transformation of leaching residue into hematite.

ACKNOWLEDGMENTS

The authors express the sincere appreciation to the financial support of the National Natural Science Foundation of China (Project No. 21978122 and 21566017).

CONFLICT OF INTEREST

There is no ethical/legal conflict involved in the article.

REFERENCES

1. B.W. Schipper, H.C. Lin, M.A. Meloni, K. Wansleebon, R. Heijunga, and E. Voet: *Resour. Conserv. Recycl.*, 2018, vol. 132, pp. 28–36. https://doi.org/10.1016/j.resconrec.2018.01.004.
2. A. Elshkaki, T.E. Graedel, L. Ciacci, and B. Reck: *Glob. Environ. Chang.*, 2016, vol. 39, pp. 305–15. https://doi.org/10.1016/j.gloenvcha.2016.06.006.
3. S. Raghavan: *Int. J. Miner. Process.*, 1979, vol. 6(2), pp. 170–71. https://doi.org/10.1016/0301-7516(79)90026-7.
4. E.M. Córdoba, J.A. Muñoz, M.L. Blázquez, F. González, and A. Ballester: *Hydrometallurgy*, 2009, vol. 93(3–4), pp. 81–87. https://doi.org/10.1016/j.hydromet.2008.04.015.
5. H.R. Watling: *Hydrometallurgy*, 2013, vol. 140, pp. 163–80. https://doi.org/10.1016/j.hydromet.2013.09.013.
6. J. Zhou, Y.L. Liao, B.J. Li, and F.R. Huang: *Chem. Ind. Eng. Prog.*, 2015, vol. 34(01), pp. 252–57. https://doi.org/10.16085/j.issn.1000-6613.2015.01.045.
7. Q. Liu and Y.H. Zhang: *Miner. Eng.*, 2000, vol. 13(13), pp. 1405–416. https://doi.org/10.1016/S0892-6875(00)00122-9.
8. F. Nakhaei and M. Irannajad: *Miner. Process. Extr. Metall. Rev.*, 2018, vol. 39(2), pp. 89–124. https://doi.org/10.1080/08827508.2017.1391245.
9. P. Huang, L. Wang, and Q. Liu: *Int. J. Miner. Process.*, 2014, vol. 128, pp. 6–15. https://doi.org/10.1016/j.minpro.2014.02.004.
10. W.Q. Qin, Q. Wei, F. Jiao, N. Li, P.P. Wang, and L.F. Ke: *Int. J. Min. Sci. Technol*, 2012, vol. 22(3), pp. 345–49. https://doi.org/10.1016/j.ijmst.2012.04.011.
11. J. Esmaeil and G. Ahmad: *Hydrometallurgy*, 2017, vol. 171, pp. 333–43. https://doi.org/10.1016/j.hydromet.2017.06.011.
12. A.G.R. Toledo, S.P. Tayar, F.A. Arena, A.V. Benedetti, and D. Bevilaqua: *Miner. Eng.*, 2022, vol. 180, p. 107467. https://doi.org/10.1016/j.mineng.2022.107467.
13. B.V. Ali, N. Sabereh, and D. Esmaeel: *Miner. Eng.*, 2022, vol. 175, p. 107281. https://doi.org/10.1016/j.mineng.2021.107281.
14. P. Sandeep, A. Ata, P. Nilotpala, and D. Haci: *Bioresour. Technol.*, 2015, vol. 196, pp. 694–706. https://doi.org/10.1016/j.biortech.2015.08.064.
15. C.L. Brierley: *Hydrometallurgy*, 2010, vol. 104(3–4), pp. 324–28. https://doi.org/10.1016/j.hydromet.2010.03.021.
16. E.M. Cordoba, J.A. Munoz, M.L. Blazquez, F. Gonzalez, and F. Ballester: *Miner. Eng.*, 2009, vol. 22, pp. 229–35. https://doi.org/10.1016/j.mineng.2008.07.004.
17. R.P. Hackl, D.B. Dreisinger, E. Peters, and J.A. King: *Hydrometallurgy*, 1995, vol. 39, pp. 25–48. https://doi.org/10.1016/0304-386X(95)00023-A.
18. Y.J. Xian, S.M. Wen, J.S. Deng, Q. Liu, and J. Nie: *Can. Metall. Q.*, 2013, vol. 51, pp. 133–40. https://doi.org/10.1179/1879139512Y.0000000001.
19. T.S. Qiu, G.H. Nie, J.F. Wang, and L.F. Cui: *Trans. Nonferrous Met. Soc. China*, 2007, vol. 17, pp. 418–22. https://doi.org/10.1016/S1003-6326(07)60108-3.
20. J.J. Wu, J. Ahn, and J. Lee: *Miner. Process. Extr. Metall. Rev.*, 2020, vol. 2, pp. 1–8. https://doi.org/10.1080/08827508.2020.1795850.
21. W.U. Sf, C.R. Yang, W.Q. Qin, F. Jiao, J. Wang, and Y.S. Zhang: *Trans. Nonferrous Met. Soc. China*, 2015, vol. 25, pp. 4110–18. https://doi.org/10.1016/S1003-6326(15)64062-6.
22. M.B. Syott, H.R. Watling, P.D. Franzmann, and D. Sutton: *Miner. Eng.*, 2000, vol. 13, pp. 1117–27. https://doi.org/10.1016/S0892-6875(00)00095-9.
23. J. Chaidez, J. Parga, J. Valenzuela, R. Carrillo, and I. Almaguer: *Metal*, 2019, vol. 9(2), p. 189. https://doi.org/10.3390/met9020189.
24. A.A. Baba, M.K. Ghosh, S.R. Pradhan, D.S. Rao, A. Baral, and F.A. Adekola: *Trans. Nonferrous Met. Soc. China*, 2014, vol. 24, pp. 1587–95. https://doi.org/10.1016/S1003-6326(14)63229-5.
25. R.G. Mcdonald and D.M. Muir: *Hydrometallurgy*, 2007, vol. 86, pp. 191–205. https://doi.org/10.1016/j.hydromet.2006.11.015.
26. L.L. Godirilwe, R.S. Magwaneng, S. Riku, H. Kazutoshi, B. Altansukh, A. Shogo, K. Takashi, M. Hidekazu, M. Kohei, K. Masanobu, and S. Atsushi: *Miner. Eng.*, 2021, vol. 173, p. 107181. https://doi.org/10.1016/j.mineng.2021.107181.
27. Y.Y. Wang, H.F. Yang, G. Zhang, J.X. Kang, and C.L. Wang: *Chem. Eng. J. Adv.*, 2020, vol. 3, pp. 100023–24. https://doi.org/10.1016/j.ceja.2020.100023.
28. J.G. Ryu: *J. Hazard. Mater.*, 2022, vol. 427, pp. 128283–85. https://doi.org/10.1016/j.jhazmat.2022.128283.
29. Y.L. Bai, W. Wang, F. Xie, D.K. Lu, and K.X. Jiang: *Trans. Nonferrous Met. Soc. China*, 2022, vol. 32, pp. 1650–63. https://doi.org/10.1016/S1003-6326(22)65900-4.
30. G.X. Ji, Y.L. Liao, Y. Wu, J.J. Xi, and Q.F. Liu: *J. Sustain. Metall.*, 2022, vol. 8, pp. 964–77. https://doi.org/10.1007/s40831-022-00561-5.
31. G. Owusu, D.B. Dreisinger, and E. Peters: *Hydrometallurgy*, 1995, vol. 38(3), pp. 315–24.
32. B. Han, B. Altansukh, K. Haga, and Y. Takasaki: *J. Sustain. Metall.*, 2017, vol. 3, pp. 528–42. https://doi.org/10.1007/s40831-017-0135-3.
33. M. Chu, C.X. Li, P. Zhang, W.B. Ji, C. Wei, Z.G. Deng, X.B. Li, G. Fan, and M.T. Li: *Chin. J. Nonferrous Met.*, 2020, vol. 30(5), pp. 1119–30. https://doi.org/10.11817/j.ysxb.1004.0609.2020-35783.

34. C.X. Li, C. Wei, S.W. Yi, G. Fan, Z.G. Deng, X.B. Li, and M.T. Li: *Hydrometallurgy*, 2019, vol. 189, p. 105112. https://doi.org/10.1016/j.hydromet.2019.105112.
35. K.Q. Xie, X.W. Yang, J.K. Wang, J.F. Yan, and Q.F. Sheng: *Trans Nonferrous Met Soc China*, 2007, vol. 17(1), pp. 187–94. https://doi.org/10.1016/S1003-6326(07)60070-336.
36. M.C. Ruiz, J. Zapata, and R. Padilla: *Hydrometallurgy*, 2008, vol. 89(1–2), pp. 32–39. https://doi.org/10.1016/j.hydromet.2007.05.00337.
37. Z.G. Deng, F. Yang, C. Wei, B.P. Zhu, P. Zeng, X.B. Li, C.X. Li, and M.T. Li: *Trans Nonferrous Met Soc China*, 2020, vol. 30, pp. 492–500. https://doi.org/10.1016/S1003-6326(20)65229-3.
38. C.X. Li, C. Wei, Z.G. Deng, X.B. Li, G. Fan, Y.Z. Wang, S.W. Yi, and M.T. Li: *Chin. J. Nonferrous Met.*, 2018, vol. 28(3), pp. 628–36. https://doi.org/10.19476/j.ysxb.1004.0609.2018.03.23.
39. F. Kastury, W. Tang, C. Herde, M.R. Noerpel, K.G. Scheckel, and A.L. Juhasz: *J. Hazard. Mater.*, 2021, vol. 418, p. 126312. https://doi.org/10.1016/j.jhazmat.2021.126312.
40. Z. Niu, G. Li, D. He, X. Fu, W. Sun, and T. Yue: *J. Hazard. Mater.*, 2021, vol. 416, p. 125972. https://doi.org/10.1016/j.jhazmat.2021.125972.
41. R.L. Frost, R.A. Wills, M.L. Weier, A.W. Musumeci, and W. Martens: *Thermochim. Acta*, 2005, vol. 432, pp. 30–35. https://doi.org/10.1016/j.tca.2005.04.001.
42. C.X. Li, Z.G. Deng, C. Wei, G. Fan, X.B. Li, M.T. Li, and Y.Z. Wang: *Hydrometallurgy*, 2018, vol. 178, pp. 294–300. https://doi.org/10.1016/j.hydromet.2018.05.012.
43. F.X. Yang, Y.B. Xing, Z.G. Deng, C. Wei, X.B. Li, and M.T. Li: *Int. J. Chem. Reactor Eng.*, 2021, vol. 19(10), pp. 1103–113. https://doi.org/10.1515/ijcre-2021-0010.
44. Z.G. Deng, B.P. Zhu, P. Zeng, C. Wei, X.B. Li, C.X. Li, and G. Fan: *Can. Metall. Q.*, 2018, vol. 58(2), pp. 223–31. https://doi.org/10.1080/00084433.2018.1535929.
45. K. Kaplun, J. Li, N. Kawashima, and A.R. Gerson: *Geochim. Cosmochim. Acta*, 2011, vol. 75(20), pp. 5865–78. https://doi.org/10.1016/j.gca.2011.07.003.
46. S.M. Javad Koleini, V. Aghazadeh, and A. Sandström: *Miner. Eng.*, 2011, vol. 24(5), pp. 381–86. https://doi.org/10.1016/j.mineng.2010.11.008.
47. H.S. Xu, C. Wei, C.X. Li, G. Fan, Z.G. Deng, X.J. Zhou, and S. Qiu: *Sep. Purif. Technol.*, 2012, vol. 85, pp. 206–12. https://doi.org/10.1016/j.seppur.2011.10.012.